CHAPTER 3

TEMPORALLY DISTINCT TRANSLESION SYNTHESIS PATHWAYS FOR ULTRAVIOLET LIGHT-INDUCED PHOTOPRODUCTS IN THE MAMMALIAN GENOME

Piya Temviriyanukul, Sandrine van Hees-Stuivenberg, Frédéric Delbos, Heinz Jacobs, Niels de Wind and Jacob G. Jansen

DNA repair 2012: 11, 550-558

ABSTRACT

Replicative polymerases (Pols) arrest at damaged DNA nucleotides, which induces ubiquitination of the DNA sliding clamp PCNA (PCNA-Ub) and DNA damage signaling. PCNA-Ub is associated with the recruitment or activation of translesion synthesis (TLS) DNA polymerases of the Y family that can bypass the lesions, thereby rescuing replication and preventing replication fork collapse and consequent formation of double-strand DNA breaks. Here, we have used gene-targeted mouse embryonic fibroblasts to perform a comprehensive study of the *in vivo* roles of PCNA-Ub and of the Y family TLS Pols η, ι, κ, Rev1 and the B family TLS Polζ in TLS and in the suppression of DNA damage signaling and genome instability after exposure to UV light. Our data indicate that TLS Pols ι and κ and the N-terminal BRCT domain of Rev1, that previously was implicated in the regulation of TLS, play minor roles in TLS of DNA photoproducts. PCNA-Ub is critical for an early TLS pathway that replicates both strongly helix-distorting (6-4) pyrimidine-pyrimidone ((6-4)PP) and mildly distorting cyclobutane pyrimidine dimer (CPD) photoproducts. The role of Polη is mainly restricted to early TLS of CPD photoproducts, whereas Rev1 and, in particular, Polζ are essential for the bypass of (6-4)PP photoproducts, both early and late after exposure. Thus, structurally distinct photoproducts at the mammalian genome are bypassed by different TLS Pols in temporally different, PCNA-Ub-dependent and independent fashions.

INTRODUCTION

Translesion synthesis (TLS) DNA polymerases are specialized enzymes that catalyze DNA synthesis across DNA lesions that form strong impediments for processive DNA polymerases δ and ε (Guo *et al.*, 2009; Waters *et al.*, 2009). TLS DNA polymerases are found in archaea, bacteria and eukaryotes, indicating that TLS is a conserved DNA damage tolerance pathway that is beneficial for cells and organisms. Indeed, in mammalian cells with DNA damage, TLS allows completion of genome duplication prior to cell division, quenches S phase checkpoint activation mediated by the Atr/Chk1 signaling pathway, prevents gross genome instability and contributes to cell survival (Guo *et al.*, 2009; Waters *et al.*, 2009). The most important group of mammalian TLS polymerases comprises the Y family DNA polymerases Pol η, ι, κ and Rev1 and the B family DNA polymerase Polζ, which consists of a catalytic subunit Rev3 and an accessory subunit Rev7 (Guo *et al.*, 2009; Waters *et al.*, 2009). The ability of Y family DNA polymerases to insert a nucleotide opposite the DNA lesion results from various atypical properties, including unusual polymerization mechanisms, the lack of an induced fit upon nucleotide binding and the absence of 3'-to-5' exonuclease activity, required for proofreading (Guo *et al.*, 2009; Waters *et al.*, 2009). Accordingly, a Y family DNA polymerase frequently inserts an incorrect nucleotide opposite the damaged nucleotide. Nucleotides inserted by the Y family Pols are excellent substrates for extension by Polζ. Like the Y family DNA polymerases, Polζ lacks proofreading activity, implicating that TLS is an inherently error-prone process that contributes significantly to spontaneous and genotoxin-induced mutagenesis (Guo *et al.*, 2009; Waters *et al.*, 2009).

Although the precise mechanism of DNA damage bypass by TLS DNA polymerases is not fully understood, mono-ubiquitination at lysine (K) 164 of the DNA sliding clamp Proliferating Cell Nuclear Antigen (PCNA-Ub) is thought to be an important event to elicit TLS (Arakawa *et al.*, 2006; Hoege *et al.*, 2002; Kannouche *et al.*, 2004; Langerak *et al.*, 2007; Stelter *et al.*, 2003; Watanabe *et al.*, 2004). Indeed, cells expressing mutant PCNA that cannot be ubiquitinated at K164 ($PCNA^{K164R}$) show impaired recruitment of TLS DNA polymerases *in vivo*, display aberrant DNA synthesis and delayed cell cycle progression, and increased sensitivity, following exposure to different genotoxic agents (Hendel *et al.*, 2011; Hoege *et al.*, 2002; Krijger *et al.*, 2011; Niimi *et al.*, 2008; Sabbioneda *et al.*, 2008). PCNA-Ub improves the physical interaction of this sliding clamp with Y family TLS DNA polymerases via specific domains located at their C-termini (Bienko *et al.*, 2005; Waters *et al.*, 2009).

Many *in vitro* studies on the function of individual TLS DNA polymerases of higher eukaryotes show that these enzymes exhibit overlapping substrate specificities (Waters *et al.*, 2009). Moreover, the *in vivo* function of TLS polymerases has been extensively addressed using chicken and mammalian cell lines with defects in individual TLS polymerases (Auclair *et al.*, 2010; Edmunds *et al.*, 2008; Gueranger *et al.*, 2008; Okada *et al.*, 2005; Petta *et al.*, 2008; Shachar *et al.*, 2009; Simpson *et al.*, 2003; Szuts *et al.*,

2008; Yoon *et al.*, 2010; Ziv *et al.*, 2009). However, the relative *in vivo* contribution of each vertebrate TLS DNA polymerase in TLS and DNA damage responses to specific genomic lesions is difficult to assess, despite the considerable progress that has been made in recent years. This difficulty is mainly due to the use of (i) cell lines of different origins which complicates comparisons of data (Gueranger *et al.*, 2008; Hendel *et al.*, 2011; Jansen *et al.*, 2009a; Jansen *et al.*, 2005; Krijger *et al.*, 2011; Okada *et al.*, 2005; Petta *et al.*, 2008; Yoon *et al.*, 2010; Ziv *et al.*, 2009), (ii) RNA interference techniques that may not completely silence the expression of the TLS polymerase of interest (Yoon *et al.*, 2010; Ziv *et al.*, 2009), (iii) cells that display an atypical phenotype in somatic hypermutation, a TLS-dependent process operating at the variable regions of immunoglobulin genes (Faili *et al.*, 2002; Gueranger *et al.*, 2008; McDonald *et al.*, 2003; Simpson *et al.*, 2003), and (iv) episomal DNA templates with site-specific lesions, which may not be fully representative of DNA damage in chromatinized genomic DNA (Shachar *et al.*, 2009; Szuts *et al.*, 2008; Yoon *et al.*, 2010; Ziv *et al.*, 2009).

UV light is a well characterized skin mutagen and carcinogen, inducing strongly helix-distorting (6-4) pyrimidine–pyrimidone ((6-4)PP) photoproducts as well as mildly distorting cyclobutane pyrimidine dimers (CPDs) (Ikehata *et al.*, 2011). These lesions obstruct processive DNA polymerases and, consequently, are substrates for TLS polymerase-mediated bypass. Here, we report on an integrative approach to study the involvement of key TLS polymerases, and of PCNA-Ub for TLS across CPDs and (6-4) PPs in genomic DNA and for DNA damage signaling, cell cycle progression, genome stability and cell proliferation. We used a defined cell type, *i.e.* mouse embryonic fibroblasts (MEFs), with defined deletions in the Y family DNA Pols η, ι, κ and Rev1 as well as in Rev3, the catalytic subunit of the B family DNA Polζ. In addition, we used MEF lines with a mutant PCNA that cannot be ubiquitinated ($PCNA^{K164R}$) or with a deletion of the N-terminal BRCT region of Rev1. This domain is involved in regulating a mutagenic TLS pathway that operates early after UV treatment (Jansen *et al.*, 2009a; Jansen *et al.*, 2005). To adequately compare the different cellular responses, we performed most experiments with the same UV dose. We report both common and quantitatively and temporally distinct roles for PCNA-Ub, Polη, Rev1 and Rev3 in different TLS pathways across both photoproducts *in vivo*, thereby extinguishing DNA damage signaling, preventing gross genome instability and protecting against cytotoxicity.

RESULTS

TLS Polymerases Differentially Contribute to UVC Toxicity

To compare the involvement of individual TLS polymerases and of PCNA modification in cellular responses to UVC light, we exposed MEFs that contained a defect either in each TLS polymerase or in PCNA modification ($PCNA^{K164R}$) to different doses of UVC light and measured cell proliferation. Compared to wild type MEFs, the MEF line defective for Rev3 was extremely sensitive to UVC, indicating an indispensable

function of Rev3 in protecting against UVC-induced cytotoxicity (Fig. 1). PCNA^{K164R} MEFs as well as MEFs deficient for Polη or Rev1 displayed moderate sensitivity to UVC. PCNA-Ub is important for recruitment of TLS polymerases to sites of DNA damage (Hendel *et al.*, 2011; Krijger *et al.*, 2011). Therefore, the UVC sensitivity of PCNA^{K164R} MEFs may be due to the difficulty in activating TLS polymerases that function in PCNA-Ub-dependent TLS across photoproducts. MEF lines deficient for Polκ, Polι and the N-terminal BRCT region of Rev1 (Rev1BRCT MEFs) were only slightly more sensitive to UVC compared to wild type MEFs, indicating that Polκ, Polι and the BRCT domain of Rev1 are mostly dispensable for tolerance to UV light. All together, these data reveal marked differences in the contribution of individual TLS proteins and of PCNA modification in protection toward cytotoxicity induced by UVC light.

Activation of DNA Double Strand Break (DSB) Response Proteins in TLS-deficient and PCNA-Mutant Cells Exposed to UVC

To obtain mechanistic insight in the different sensitivities of the TLS-defective MEF lines to UVC, we performed immunoblotting to investigate phosphorylation of histone H2AX at S139 (γ-H2AX) and of KRAB-ZFP–associated protein 1 at S824 (KAP1^{S824-P}), that may reflect the induction of both ssDNA and DSBs (de Feraudy *et al.*, 2010; Rogakou *et al.*, 1998; White *et al.*, 2006; Ziv *et al.*, 2006). As shown in Figs. 2A and B, following exposure to 5 J/m^2 UVC, all tested cell lines displayed similar kinetics of γ-H2AX accumulation, *i.e.* γ-H2AX was detectable already 2h after treatment and levels gradually increased to a maximum at 24-36h. Yet, the absolute levels of γ-H2AX

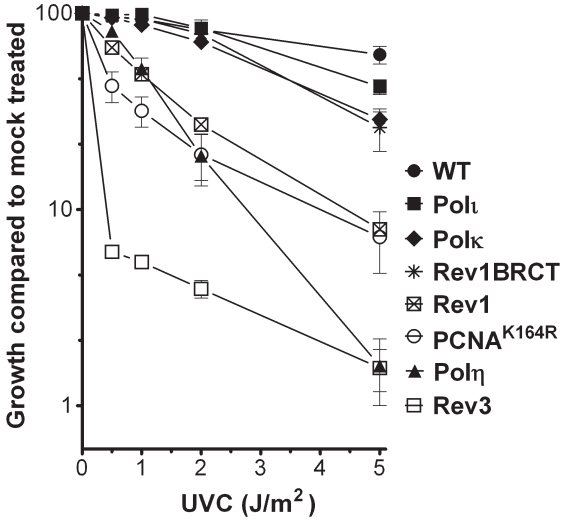

Figure 1 | Effect of UVC on the proliferation of MEFs with defined defects in TLS-related genes. Cells were treated with various doses of UVC. After 3 days, the number of cells was determined. The number of unexposed cells was set at 100% to calculate relative cell growth. Error bar, SD (*n*=3).

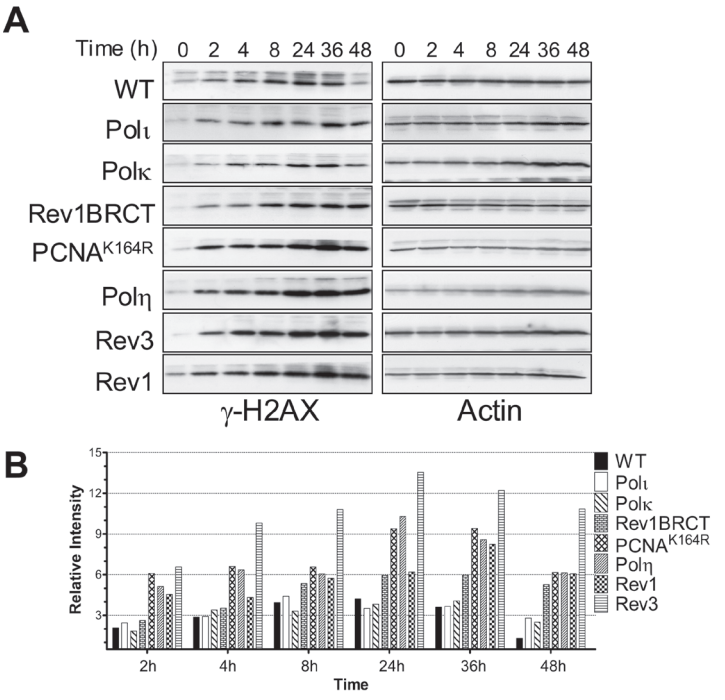

Figure 2 | Effect UVC on formation of γ-H2AX in MEFs with defined defects in TLS-related genes. Whole cell extracts prepared at different times after exposure to UVC (5 J/m^2) were used for western blot analysis. 0h: cell extract prepared instantly after exposure. (A) Blots representing expression of γ-H2AX (left panel) and β-actin (right panel). (B) Quantification of γ-H2AX upon UVC exposure relative to the loading control β-actin.

differed considerably among the cell lines. MEFs deficient for Polι or Polκ showed almost no difference in the formation of γ-H2AX as compared to wild type MEFs, in concordance with their moderate sensitivities to UVC. The Rev1BRCT MEFs displayed an intermediate increase in γ-H2AX levels. The highest induction of γ-H2AX was found for MEFs deficient in Rev3. Also PCNA^{K164R} MEFs and MEFs deficient in Rev1 or in Polη displayed a pronounced induction of γ-H2AX, peaking at 24-36h after UVC treatment. Accumulation of KAP1^{S824-P} coincided with that of γ-H2AX in most cell lines (Figs. 2A, B and S1). Together, these results suggest that the sensitivities of TLS-defective MEF lines correlate with the induction of DNA breaks.

UVC Induces Genome Instability in Rev1, Rev3, Polη and PCNA-Ub Mutants

The induction of DSBs can be directly measured by analyzing the formation of micronuclei using the cytokinesis-blocked micronuclei assay (Fenech, 1993). In this assay, the use of the cytokinesis inhibitor cytochalasin B results in the accumulation of binucleated, post-mitotic, cells. Here, we have determined the formation of micronuclei in such post-mitotic, TLS-defective or PCNA-mutant, MEFs after UVC

exposure. Since insufficient numbers of binucleated cells were obtained to reliably determine micronuclei formation in some of the MEF lines after exposure to 5 J/m^2 UVC, we set out to determine micronuclei using equitoxic doses of UVC that lead to 30% cell survival for all MEF lines. After normalization for the different UVC doses, to relate the frequencies of micronuclei to photolesion densities, the highest frequencies of micronuclei were found in PCNA^{K164R}, Rev1- and Rev3-deficient MEFs (Fig. 3). These data indicate that PCNA-Ub, Rev1 and, in particular, Rev3 are very important in preventing genome instability following UVC exposure

Differential Involvement of TLS Polymerases and PCNA Modification in TLS Across UVC-Induced DNA Damages

The formation of DSBs might reflect collapsed replication forks after their stalling at photoproducts. Such stalling results in persistent ssDNA ends, either opposite the lesion, or downsteam of the lesion, where processive replication may have reprimed. To measure persistent ssDNA ends, we employed the alkaline DNA unwinding (ADU) assay. Compared to mock treatment, in wild type MEFs, Rev1BRCT MEFs and MEFs deficient for Polι or Polκ, replication fork progression recovered to rates similar to mock-treated cells beyond 4h after treatment (Fig. 4). This result indicates that Pols ι and κ and the N-terminal BRCT region of Rev1 do not play a major role in bypass of genomic photoproducts. Conversely, compared with wild type MEFs, Polη-deficient MEFs displayed pronounced persistence of ssDNA during the first 2h after UVC exposure, whereas at later times maturation of nascent DNA slowly recovered (Fig. 4). Also PCNA^{K164R} MEFs displayed a slow recovery of DNA maturation following an initial delay that was less pronounced than the delay in

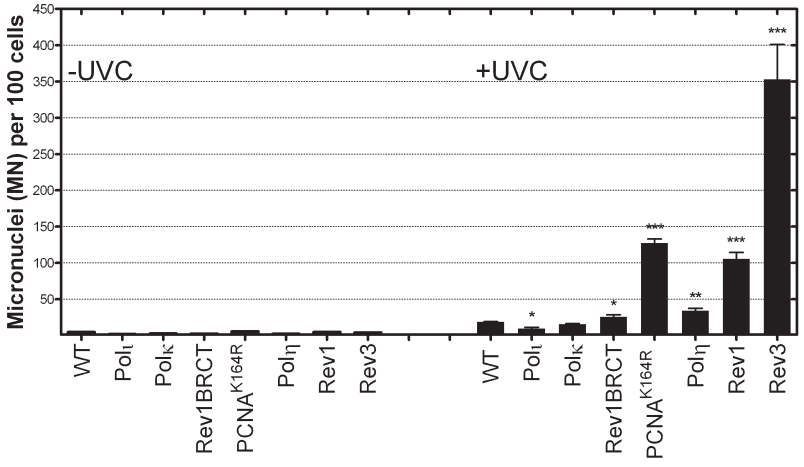

Figure 3 | Frequencies of UVC-induced micronuclei (MN) in MEFs with defined defects in TLS-related genes. MN induction in binucleated cells, fixed 24 h after cyt-B treatment, was determined in MEFs exposed to a dose of UVC resulting in 30% cell survival. The frequencies of MN were corrected for the doses used. Bars represent the number of MN per 100 cells after exposure to UVC or mock treatment (n=3). Error bar, SEM. Statistical significance was analyzed by Student's t-test against treated WT. **, p<0.01; ***, p<0.001.

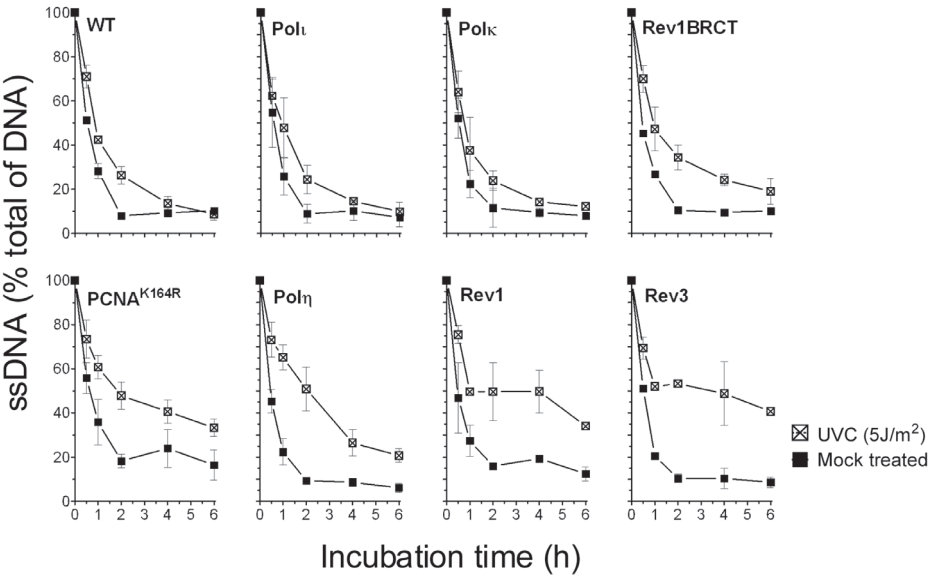

Figure 4 | Relative inhibition of replication fork progression upon UVC exposure in MEFs with defined defects in TLS-related genes. Replication fork progression in different MEF lines was measured up to 6h upon UVC exposure (5 J/m^2) or mock treatment (n=3). The amount ssDNA (% total DNA) is related to stalled replication forks and was set at 100% at 0h. Error bar, SD.

the Polη-deficient cells. Together these data suggest that in these cell lines an alternative, PCNA-Ub-independent, pathway completes synthesis of most, albeit not all, nascent DNA. In contrast, maturation of nascent DNA was almost completely abolished in MEFs deficient for Rev1 or Rev3, already after 1h following UVC exposure (Fig. 4). This result signifies that Rev1 and Rev3 are essential for replicative bypass at photoproducts and may act independently from PCNA-Ub and Polη.

Activation of DNA Damage Signaling is Correlated with Defects in Photoproduct Bypass

Upon the generation of ssDNA, the essential DNA damage signaling kinase Atr phosphorylates the serine/threonine kinase Chk1 (Smits *et al.*, 2010). To test whether the observed differences in replication fork progression among the various UV-exposed MEF lines correlate with the extent of Atr activation, we determined the levels of Chk1, phosphorylated at Serine (S) 345 (Chk1$^{S345\text{-}P}$), in UV-exposed cells, using immunoblotting. Within 8h after 5 J/m^2 UVC treatment, rapid and robust induction of Chk1$^{S345\text{-}P}$ was observed in MEFs deficient for Polη, Rev1 and Rev3 as well as for PCNA^{K164R} MEFs (Fig. 5), the same cell lines that display significant defects in replication fork progression. Wild type MEFs and MEFs deficient for Polι showed only weak induction of Chk1$^{S345\text{-}P}$ in response to UVC, whereas MEFs defective in Polκ or Rev1BRCT MEFs displayed moderate Chk1$^{S345\text{-}P}$ signals. Of note, phosphorylation

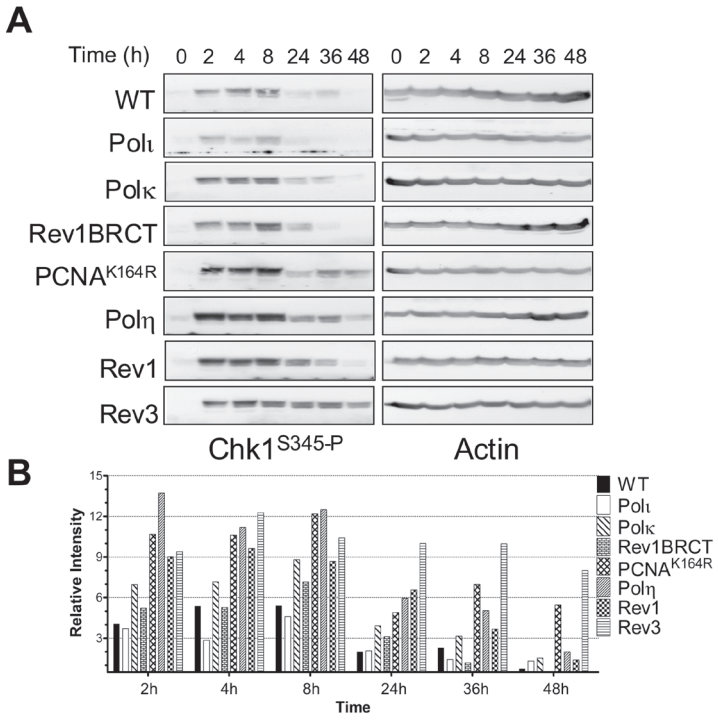

Figure 5 | Effect of UVC on DNA damage checkpoint responses in MEFs with defined defects in TLS-related genes. Whole cell extracts prepared at different times after exposure to UVC (5 J/m^2) were used for Western blot analysis. 0h: cell extract prepared instantly after exposure. (A) Blots representing expression of Chk1$^{S345\text{-}P}$ (left panel) and β-actin (right panel). (B) Quantification of Chk1$^{S345\text{-}P}$ upon UVC exposure relative to the loading control β-actin.

of Chk1 maximizes much earlier than that of KAP1 and H2AX, suggesting that DSBs originate from persisting ssDNA regions (Figs. 2 and 5).

Different TLS Mutants are Differentially Affected in S Phase Progression After UVC Exposure

To relate the extent of replication fork stalling with the induction of cell cycle responses, we determined cell cycle progression of the cells pulse-labeled during S phase with BrdU, immediately after UVC exposure (Figs. 6 and S2A–D). At 4h after labeling, all mock-treated MEF lines displayed the appearance of BrdU-positive cells in the subsequent G1 phase, indicating that cell cycle progression of undamaged MEF lines was not affected by the TLS defects (Fig. S2D). Compared to untreated cell populations, treatment with 5 J/m^2 UVC induced only mild delays in cell cycle progression in wild type MEFs and in MEFs deficient for Polι, Polκ and Rev1BRCT (Figs. 6 and S2D). Polη-deficient MEFs, however, displayed a much stronger accumulation during mid-S phase (Fig. 6). In contrast to Polη-deficient MEFs, UV-exposed PCNA^{K164R} MEFs progressed

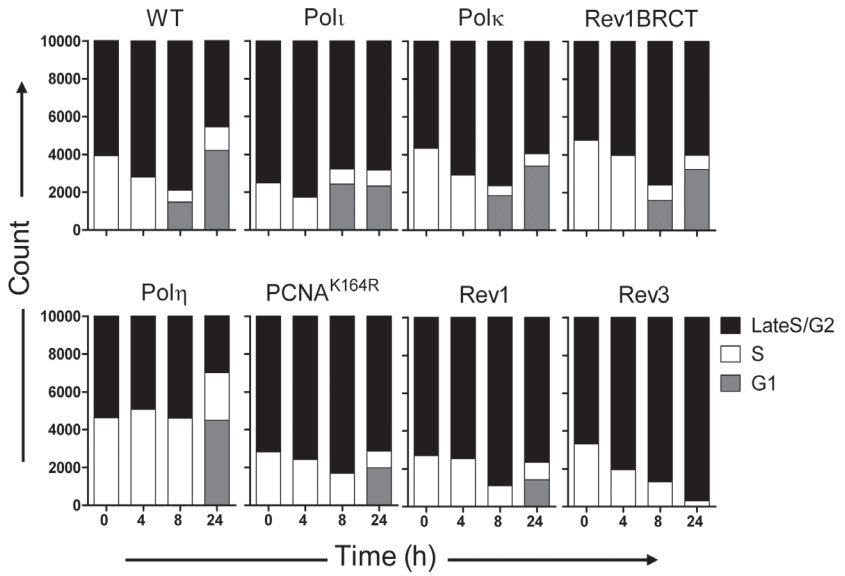

Figure 6 | Cell cycle progression of MEFs with defined defects in TLS-related genes. Cells were pulse-labeled with BrdU, immediately after UVC exposure (5 J/m^2). Then, BrdU-positive cells in G1, S and late S/G2 phases were quantified, at different times up to 24h after treatment.

more rapidly through the S phase, accumulating only at the late S/G_2 phase (Fig. 6). This result may indicate that Polη plays an early role in TLS, independent of PCNA-Ub, a hypothesis that is consistent with the more pronounced defect in replication fork progression of the Polη-deficient MEFs, as measured by the ADU assay (Fig. 4). Similar to PCNA^{K164R} MEFs, MEFs deficient for Rev1 or Rev3 strongly accumulated only at the late S/G_2 phase, following UVC exposure. All UV-exposed mutant MEF lines were capable of entering a new cell cycle, except Rev3-deficient MEFs that arrested indefinitely at the G_2-phase (Fig. 6).

Identification of Genomic Substrates for PCNA-Ub and Individual TLS Polymerases

The prolonged formation of Chk1^{S345-P} in PCNA^{K164R} MEFs and MEFs defective for Polη, Rev1 and Rev3 after UVC exposure (Fig. 5) suggests the persistence of ssDNA containing photoproducts following replication fork stalling. We recently described an innovative approach to identify the specific genomic photoproducts that are substrates for individual TLS polymerases. This approach depends on immunostaining of non-denatured DNA using monoclonal antibodies that recognize either (6-4)PPs or CPDs, embedded in ssDNA (Jansen *et al.*, 2009a; Jansen *et al.*, 2009b). Here, we further developed this method to compare the timing and substrate specificities for Rev1, Polη- and PCNA-Ub-mediated DNA damage bypass in replicating cells. Thus, MEFs were exposed to 5 J/m^2 UVC and pulse-labeled with EdU, enabling to identify cells that were replicating during UVC exposure. These cells were fixed and stained under

non-denatured conditions for EdU and for CPD or (6-4)PP, after UVC treatment. Wild type MEFs were included as controls. Neither CPDs nor (6-4)PPs were detected in wild type MEFs at 2h or 8h after UVC treatment, suggesting efficient replication across both genomic lesions (Fig. 7). In contrast, in nuclei of EdU-positive MEFs deficient for Polη, unreplicated CPDs were clearly detectable at 2h after UVC exposure whereas at 8h staining for CPDs was strongly reduced (Fig. 7). Since CPDs are hardly repaired in mouse cells (Van Sloun *et al.*, 1999; Yagi *et al.*, 1984), these results suggest that Polη is mainly involved in an early bypass pathway at CPDs. Moreover, in Polη-deficient MEFs a backup pathway most likely replicates CPDs at a later stage. Also PCNA^{K164R} MEFs stained positive for unreplicated CPDs although the staining persisted much longer than in the Polη-deficient MEFs. This indicates that PCNA-Ub directs a Polη-independent bypass pathway for CPDs, late after exposure. Little staining of CPD in ssDNA was detected in nuclei of replicating Rev1-deficient MEFs, in agreement with previous results (Jansen *et al.*, 2009a). In contrast, strong staining of (6-4)PPs in ssDNA was seen in Rev1-deficient MEFs that were replicating during UV treatment, both early and late after UVC exposure. As we have previously excluded that Rev1 plays a role

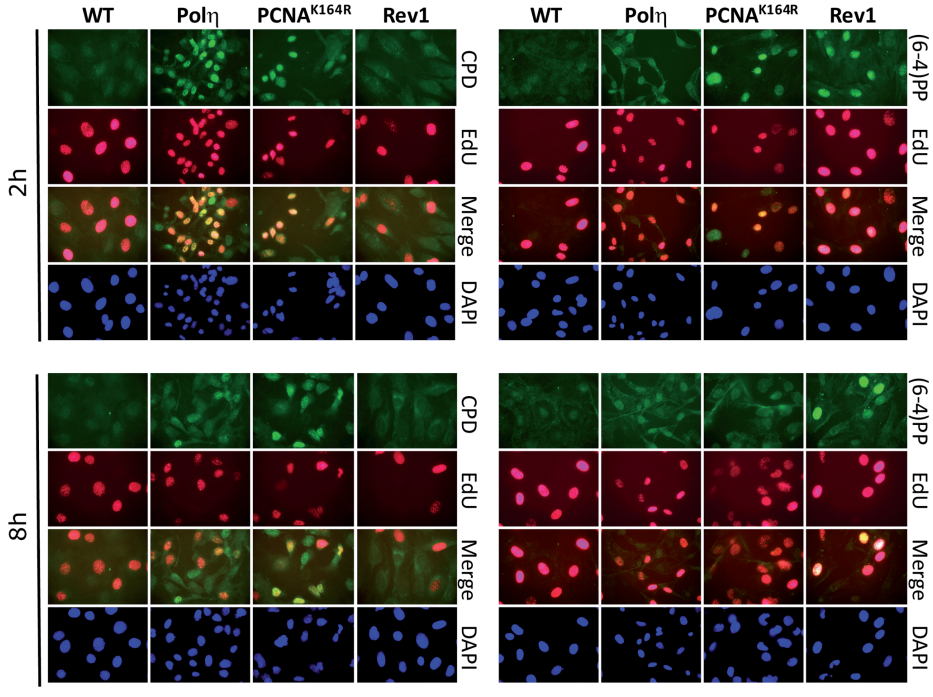

Figure 7 | Different substrate specificities and kinetics of photoproduct bypass for Polη, PCNA-Ub and Rev1. Cells were exposed to 5 J/m^2 UVC and immediately pulse-labeled with EdU. Cells were fixed 2h (upper panels) and 8h (lower panels) and immunostained for CPDs (green, left panels) or for (6-4)PPs (green, right panels) in ssDNA of nuclei (DAPI, blue) in replicating (EdU-positive, red) and non-replicating cells at the time of UVC exposure. Merge represents combined stainings for UV lesions and for EdU.

in nucleotide excision repair of (6-4)PPs (our unpublished data), this result confirms previous data suggesting that Rev1 acts both early and late to bypass (6-4)PPs (Jansen *et al.*, 2009a). This result also demonstrates that there is no backup pathway for the bypass of (6-4)PP. Interestingly, PCNA^{K164R} MEFs and, to a minor extent, Polη-deficient MEFs displayed accumulation of unreplicated (6-4)PPs, in the case of PCNA^{K164R} MEFs only early after UV exposure (Fig. 7). This result indicates that both PCNA-Ub and Rev1 are essential for the early bypass of (6-4)PPs, while a Rev1-dependent but PCNA-Ub-independent pathway replicates (6-4)PPs, late after UVC exposure. We noted that some cells that stained positive for UV-damages within ssDNA were EdU-negative. Most likely, these cells had entered S phase after pulse-labeling with EdU. Conversely, EdU-positive MEFs that showed no staining for photolesions in ssDNA, early after UV exposure, were probably labeled with EdU during the end of S phase, precluding the accumulation of stalled replication forks.

DISCUSSION

In this study, we have determined the contribution of all five key mammalian TLS polymerases, and PCNA modification at K164, in replication fork progression, DNA damage signaling, cell cycle progression and genome stability *in vivo*, in response to UVC exposure.

MEF lines defective for Pols ι, κ and the BRCT region of Rev1 displayed very mild phenotypes, indicating that these factors play only minor roles in TLS across genomic photolesions *in vivo*. In support, purified human Polκ is not able to insert nucleotides opposite CPDs and (6-4)PP (Zhang *et al.*, 2000), although there is evidence that Polι and Polκ can act as backups to Polη on a site-specific CPD-containing plasmid (Ziv *et al.*, 2009). Alternatively, the minor UV sensitivity of Polκ-deficient MEFs might be caused by a defect in gap filling during nucleotide excision repair of (6-4)PP (Ogi *et al.*, 2006; Ogi *et al.*, 2010). Polι might be involved in bypassing some (6-4)PPs, as indicated by the analysis of (6-4)PP-induced mutations at episomal vectors in cells treated with Polι siRNA (Yoon *et al.*, 2010). Since Polι plays a significant role in responses to oxidative stress (Petta *et al.*, 2008; Temviriyanukul *et al.*, 2012), it might be that Polι protects cells from cytotoxicity induced by long-wave UVA light that, in contrast with UVC, induces oxidative DNA damage. Nevertheless, deficiencies for Pols ι, κ and the Rev1BRCT region may still lead to significant damage responses and biological effects under specific conditions (Dumstorf *et al.*, 2006; Ohkumo *et al.*, 2006; Tsaalbi-Shtylik *et al.*, 2009; Yoon *et al.*, 2010; Ziv *et al.*, 2009).

MEFs deficient for Polη, Rev1 and Polζ, as well as the PCNA^{K164R} mutant, displayed significant defects in responses to DNA photolesions, albeit in quantitatively and qualitatively different fashions. In Polη-deficient cells, we found a defect in TLS at genomic CPDs predominantly early after UVC treatment. Polη-dependent TLS at CPDs quenches Chk1 signaling (Fig. 5) and prevents the accumulation of cells during

mid-S phase (Fig. 6) and genome instability (Figs. 2 and 3). Indeed, Polη is considered to be the principal TLS polymerase for CPDs and other moderately helix-distorting lesions (Yoon *et al.*, 2010; Ziv *et al.*, 2009). In Polη-deficient cells the delayed bypass of CPDs (Figs. 4 and 7) may be mediated by Pols ι, κ and ζ, albeit at the expense of higher mutation rates (Ito *et al.*, 2012; Yoon *et al.*, 2010; Ziv *et al.*, 2009). However, since these putative backup pathways are unable to rescue the Polη defect completely (Fig. 4), some stalled forks will ultimately collapse, resulting in the formation of cytotoxic DSBs in the absence of Polη (Figs. 1–3).

Similar to Polη, PCNA-Ub is involved in TLS of CPDs. However, compared with Polη-deficient MEFs, $PCNA^{K164R}$ mutant MEFs displayed less delay in fork progression early after UVC treatment (Fig. 4) and a less pronounced S phase arrest (Fig. 6). These data suggest that Polη may partially operate independently of PCNA-Ub during TLS of CPDs, in agreement with previous observations (Hendel *et al.*, 2011; Krijger *et al.*, 2011; Schmutz *et al.*, 2010). Notably, in a previous study we showed that $PCNA^{K164R}$ pre-B cells progressed somewhat slower through S phase compared with Polη-deficient pre-B cells (Hendel *et al.*, 2011; Krijger *et al.*, 2011). In comparison with the present study, this different result may reflect cell type-specific dissimilarities and stresses the importance of our integrative approach to study DNA damage bypass, DNA damage responses and the induction of genome instability in a defined cell type.

Surprisingly, in addition to a defect in TLS of CPDs, $PCNA^{K164R}$ and, to a minor extent, Polη-deficient MEFs displayed also a defect in the bypass of genomic (6-4)PP (Fig. 7). The greater dependence of (6-4)PP bypass on PCNA-Ub than on Polη may explain the higher induction of DSBs in the PCNA-Ub-mutant cells compared with the Polη-deficient cells (Fig. 3). The nature of this pathway is elusive, although Rev1 and Polζ may be involved (Hendel *et al.*, 2011).

Compared with Polη and PCNA-Ub-defective MEFs, Rev1 or Rev3-deficient MEFs displayed different responses to UVC exposure: (i) Replication fork progression shortly after UVC exposure is less inhibited in Rev1 or Rev3-deficient MEFs (Fig. 4). This difference may reflect the observed dissimilarities in substrate specificities (Fig. 7), since Polη and PCNA-Ub act primarily on abundant CPDs, whereas *in vivo* Rev1 and Rev3 mainly operate on, less abundant, (6-4)PPs (Jansen *et al.*, 2009a; Jansen *et al.*, 2009b). (ii) Replication forks stalled at (6-4)PP remain obstructed for a long time in MEFs deficient for Rev1 or Polζ, indicating that in contrast to CPDs no backup pathway exists for bypass of (6-4)PP (Figs. 4 and 7; (Jansen *et al.*, 2009a; Jansen *et al.*, 2009b; Szuts *et al.*, 2008)). Importantly, this result additionally suggests that (6-4)PP at stalled forks are refractory to repair by NER, contradicting models describing the repair of DNA damage following regression of the stalled replication fork (Atkinson *et al.*, 2009). Moreover, Rev1 and Rev3 strongly suppress the formation of DSBs in mammalian cells (Fig. 3; (Van Sloun *et al.*, 2002; Wittschieben *et al.*, 2006)) by catalyzing TLS and, possibly, by promoting homologous recombination to repair DSBs (Sharma *et al.*, 2012). Furthermore, the much stronger defect in (6-4)PP bypass of MEFs deficient for Rev1 or Polζ than of $PCNA^{K164R}$

MEFs, at 8h after UV exposure, suggests that in mammalian cells the late Rev1 and Polζ-dependent bypass of (6-4)PP does not depend on PCNA-Ub, similar to chicken DT40 cells (Edmunds *et al.*, 2008). (iii) Perhaps surprisingly, in contrast to Polη-deficient MEFs, MEFs deficient for Rev1 or Rev3 progress relatively normally through S phase following UVC exposure, despite accumulation of arrested replication forks, persistence of unreplicated (6-4)PP and concomitant Chk1 activation (Figs. 4–7 and Fig. S2C; (Jansen *et al.*, 2009a; Jansen *et al.*, 2009b)). Collectively, these data corroborate previous results indicating that Rev1 and Rev3 act preferentially at post-replicative gaps, rather than at the stalled replication fork itself, thereby quenching DNA damage signaling (Daigaku *et al.*, 2010; Diamant *et al.*, 2012). In agreement, we have recently described that Rev1 can be recruited to 5' phosphorylated primer-template junctions that can be generated by repriming of postreplicative replication, downstream of the unreplicated lesion (de Groote *et al.*, 2011). It has been proposed that Rev1 functions as a scaffold protein to recruit other TLS polymerases to TLS intermediates (Andersen *et al.*, 2011; Guo *et al.*, 2009; Ohashi *et al.*, 2004; Tissier *et al.*, 2004; Waters *et al.*, 2009). Most likely, Rev3 is recruited to extend 3' DNA ends generated by incorporation opposite (6-4)PP photoproducts (Shachar *et al.*, 2009). Although also Polκ may act as an extender TLS polymerase (Yoon *et al.*, 2009; Ziv *et al.*, 2009), our data suggest that in the absence of Rev3 neither Polκ nor any other polymerase acts as a backup extender polymerase during genomic DNA damage bypass in mammalian cells. Of note, the induction of high levels of micronuclei in the Rev1, Rev3 and PCNA^{K164R} mutants (Fig. 3) indicates that prolonged stalling of replication forks at (6-4)PP photoproducts is a predominant source of UV-induced DSBs.

In conclusion, we have described an integrative approach to study qualitative and quantitative aspects of TLS, DNA damage responses and the induction of genome instability in a defined cell type. This approach provides novel inroads in the study of DNA damage bypass at the mammalian genome, defining not only the individual actors but also temporally distinct bypass pathways that operate at structurally distinct lesions (Table 1). To delineate these pathways even more accurately, we are investigating MEF lines with double deficiencies in factors involved in TLS.

Table 1 | Contribution of TLS polymerases and ubiquitination of PCNA in temporally distinct bypass pathways operating at genomic CPDs or (6-4)PPs

	CPDs				**(6-4)PPs**			
	Polη	**PCNA^{K164}**	**Rev1**	**Rev3[a]**	**Polη**	**PCNA^{K164}**	**Rev1**	**Rev3[a]**
Pathway								
early	+	+	-	ND[b]	±	+	+	ND
late	-	+	-	±	±	-	+	+

[a] Taken from (Jansen *et al.*, 2009b)
[b] ND, not determined

MATERIALS AND METHODS

Cell culture. Immortalized MEFs homozygous for a targeted disruption of Rev1, the N-terminal BRCT region of Rev1 or Rev3 were described previously (Jansen *et al.*, 2006; Jansen *et al.*, 2009a; Jansen *et al.*, 2009b). MEFs lacking Polη or Polι were isolated from day 13.5 embryos of Polη or Polι deficient mice and cultured until spontaneous immortalization. Polη-deficient mice have been described previously (Delbos *et al.*, 2005). The generation of Polι-deficient mice will be described elsewhere (Aoufouchi et al., in preparation). A MEF line deficient for Polκ was kindly provided by Dr. Haruo Ohmori (Kyoto University, Japan). A MEF line homozygous for a $PCNA^{K164R}$ mutation was described previously (Krijger *et al.*, 2011). All MEF lines were cultured in Dulbecco's modified Eagle's medium (DMEM) containing 4.5g/l glucose, Glutamax and pyruvate (Invitrogen), supplemented with 10% fetal calf serum, penicillin (100U/ml), and streptomycin (100µg/ml) (DMEM medium) at 37°C in a humidified atmosphere containing 5% CO_2.

Cell proliferation assay. Per well of a 6-well plate, 5×10^4 exponentially growing cells were seeded in DMEM medium and cultured overnight. Cells were washed twice with phosphate buffer saline (PBS) before exposure to various doses of UVC light (Philips TUV lamp, predominantly 254 nm). After exposure, fresh DMEM medium was added and the cells were cultured for 3 days. Then, cells were trypsinized and counted using a Z2 coulter particle and size analyzer (Beckman coulter). At least three completely independent experiments were performed.

Western blot analysis. Per P90 dish, 10^6 cells were seeded and cultured overnight in DMEM medium. Prior to UVC exposure at 5 J/m^2, or mock treatment, cells were rinsed with PBS. After treatment, cells were cultured in DMEM medium and at the indicated times cells were lysed by adding Laemmli lysis buffer directly onto cells. Proteins were separated by SDS-PAGE and blotted onto a nitrocellulose membrane (Hybond-C extra, Amersham Biosciences). The membranes were incubated in blocking buffer (Rockland) and PBS-0.1% Tween 20 in a 1:1 ratio for at least 30 min at room temperature. Thereafter, membranes were incubated overnight with primary antibodies at 4°C and with appropriate peroxidase-conjugated secondary antibodies (Bio-Rad) for 1h at room temperature, subsequently. Proteins were visualized by enhanced chemiluminescence detection (ECL). The following antibodies were used: rabbit monoclonal anti-phospho Chk1 (S345) (Cell signaling), mouse monoclonal anti-phospho-H2AX (S139) (Millipore), mouse monoclonal anti-actin antibody (Oncogene) and rabbit polyclonal anti-phospho Kap1 (S824) (Bethyl Laboratory). At least two completely independent experiments were performed.

Cytokinesis-blocked micronucleus assay. Per P90 dish, $1.5x10^6$ cells were plated and cultured overnight in DMEM medium. Then, $7.5x10^4$ cells were seeded on a sterile glass slide (76x26 mm) and cultured overnight. Cells attached to the slide were rinsed twice with 10 ml PBS before UVC exposure, followed by further incubation. Mock treated cells were included as experimental controls. To inhibit cytokinesis, 3µg/ml of cytochalasin B (cyt-B) (Sigma-Aldrich) was added to the cells, 24h after treatment. Twenty-four hours later, cells were fixed for 15 min using a fixative solution containing 3.5% cold paraformaldehyde and 0.5% Triton-X100. Next, slides were washed thrice with ice-cold PBS and nuclei were stained with DAPI (17.5ng/ml) (Sigma-Aldrich) in the dark for 15 min. To dehydrate the cells, slides were drenched in 70%, 90% and absolute ethanol in the dark for 5 min each, respectively. The number of binucleated cells that contained one or more micronuclei was scored by using a fluorescence microscope (Zeiss, Germany) and the Metafer 4 program (Metasystem, Germany).

Alkaline DNA unwinding (ADU). This assay was slightly adapted from (Johansson *et al.*, 2004). Per well 5×10^4 cells were plated in 24-well plate in DMEM medium and cultured overnight. Then,

the cells were pulse labeled with [^{3}H]thymidine (2 μCi/ml; 76 Ci/mmol) for 15 min and rinsed once with PBS before exposure to 5 J/m^2 of UVC. At indicated times, up to 6h, cells were rinsed twice with ice-cold 0.15M NaCl and DNA was locally denatured at the DNA replication fork with ice-cold denaturation solution (0.15M NaCl and 0.03M NaOH) for 30 min. To terminate the reaction, 1 ml of ice-cold 0.02M Na_2HPO_4 was added. Before storage overnight at -20°C, the samples were sonicated and subsequently SDS was added to a final concentration of 0.25%. Lysates were thawed and loaded onto hydroxyl apatite columns to elute ssDNA (stalled forks) from dsDNA (replicated DNA) using 0.13M K_2HPO_4 and 0.3M K_2HPO_4 pH 6.8, respectively. The radioactivity in both eluates was counted by liquid scintillation counting (Perkin-Elmer).

Bivariate cell cycle analysis. Exponentially growing MEFs were plated in P90 dishes and cultured overnight. Cells were washed once with PBS and exposed to 5 J/m^2 of UVC or mock treated. After treatment, cells were pulse-labeled with 10μM Bromodeoxyuridine (BrdU, Millipore) for 30 min at 37°C in the dark. To stop the labeling reaction, cells were rinsed once with PBS and continuously cultured in DMEM medium containing 5μM Thymidine (Sigma-Aldrich). At desired time points, cells were trysinized and fixed with 70% ethanol. Before staining, cells were permeabilized by 2M HCl/0.05% Triton-X for 35 min and subsequently neutralized by 1M Tris. Neutralized cells were incubated overnight with a mouse monoclonal antibody against BrdU (Becton Dickinson) at 4°C. Consequently, cells were washed and incubated with a FITC-conjugated rat anti-mouse antibody (BD bioscience Pharmingen) for 1h at room temperature in the dark. Then, cells were centrifuged and resuspended in PBS containing 10μg/ml of Propidium Iodide and 100μg/ml of RNase A to stain genomic DNA. Finally, the cells were analyzed by flow cytometry (Guava easyCyte HT, Millipore).

Immunofluorescent detection of unreplicated CPDs and (6-4)PPs in S phase cells. Detection of CPDs or (6-4)PPs in single-stranded DNA templates was performed as previously described with major modifications (Jansen *et al.*, 2009a). MEFs cultured on coverslips were irradiated with 0 or 5 J/m^2 UVC light, followed by 30 min pulse-labeling with 10μM 5-ethynyl-2'-deoxyuridine (EdU) (Invitrogen) in the dark. Two or eight hours later, MEFs were treated with 1% Triton-X100 in PBS for 2 min and subsequently fixed in 2% Formaldehyde/PBS containing 0.5% Triton-X100 for 15 min at room temperature. EdU positive cells were visualized using AlexaFluor 647-conjugated azide following the manufacturer's recommendations (Click-iT™ Edu imaging kit - Invitrogen). Unreplicated photoproducts were identified in non-denatured DNA using primary mouse monoclonal antibodies against (6-4)PPs (64-M2, CosmoBio) or CPDs (TDM2, CosmoBio). After incubation with secondary Alexafluor488-labeled goat-anti-rat antibodies (Molecular Probes, Inc.), nuclei were stained with 4,6-diamidino-2-phenylindole (DAPI). To check the functionality of the primary antibodies, immunofluorescence was performed essentially as described above, except that after EdU detection, cells were fixed with 2% Formaldehyde and denatured with 2N HCl for 10 min. Coverslips were mounted (Vectashield, Vector laboratories) and analyzed by fluorescent microscopy.

ACKNOWLEDGEMENTS

The authors wish to thank Dr. Haruo Ohmori (Kyoto University, Japan) and Mark Drost (LUMC) for their critical comments. We also thank Anastasia Tsaalbi-Shtylik, Matty Meijers and Jan J W A Boei, Department of Toxicogenetics, LUMC, for helpful contributions in cell cycle experiments, immunostainings and the micronucleus assay. This work was supported by a PhD scholarship to Piya Temviriyanukul under the project Strategic Frontier Research (SFR-4) from Office of the Higher Education Commission, Ministry of Education, Thailand.

SUPPLEMENTARY FIGURES

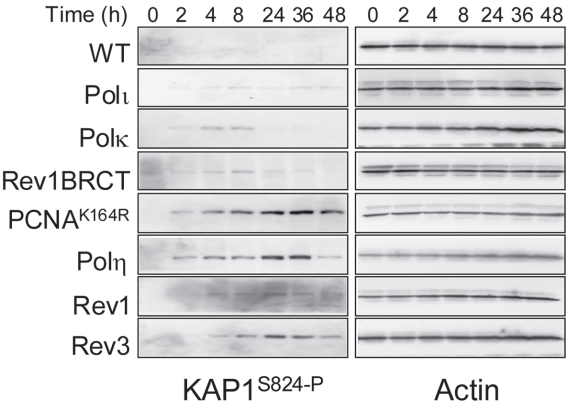

Figure S1 | Effect UVC on KAP^{S824-P} activation of MEFs with defined defects in TLS-related genes. Whole cell extracts were prepared at different times after exposure to UVC (5 J/m^2) and used for western blot analysis. 0h: cell extract prepared instantly after exposure. Blots representing expression of KAP^{S824-P} (left panel) and loading control β-actin (right panel).

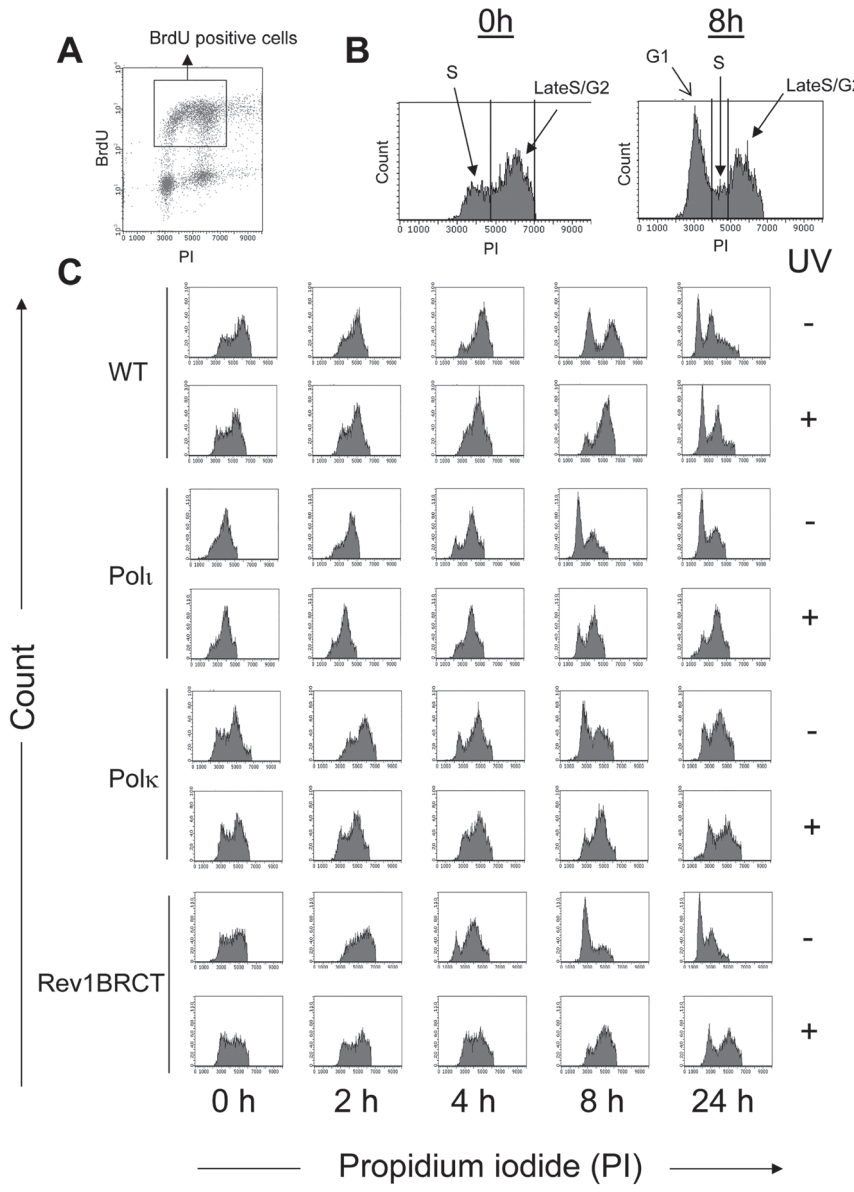

Figure S2 | Bivariate cell cycle analysis for MEFs with defined defects in TLS-related genes. Immediately after mock treatment or UVC exposure (5 J/m^2), cells were pulse-labeled with BrdU. Cells were fixed at different times up to 24h after mock or UVC treatment, stained for BrdU incorporation and DNA content (PI) and analyzed by flow cytometry. (A) Cell cycle profile of MEFs pulse-labeled with BrdU. The population of BrdU-positive cells within the area indicated by a dashed line was used for quantification. (B) Distribution of BrdU-positive cells in G1, S and late S/G$_2$ stages of the cell cycle. (C) Cell cycle profiles of BrdU-positive wild type MEFs (WT) and various MEF lines containing targeted mutations in TLS-related genes (Polι, κ, η, PCNA^{K164R}, Rev1BRCT, Rev1, Rev3) at 0, 2, 4, 8 and 24h after mock treatment (-UV) or exposure to 5 J/m^2 UVC (+UV). (D) Quantification of BrdU-positive cells in G1, S and late S/G$_2$ phases at different times up to 24h after mock treatment.

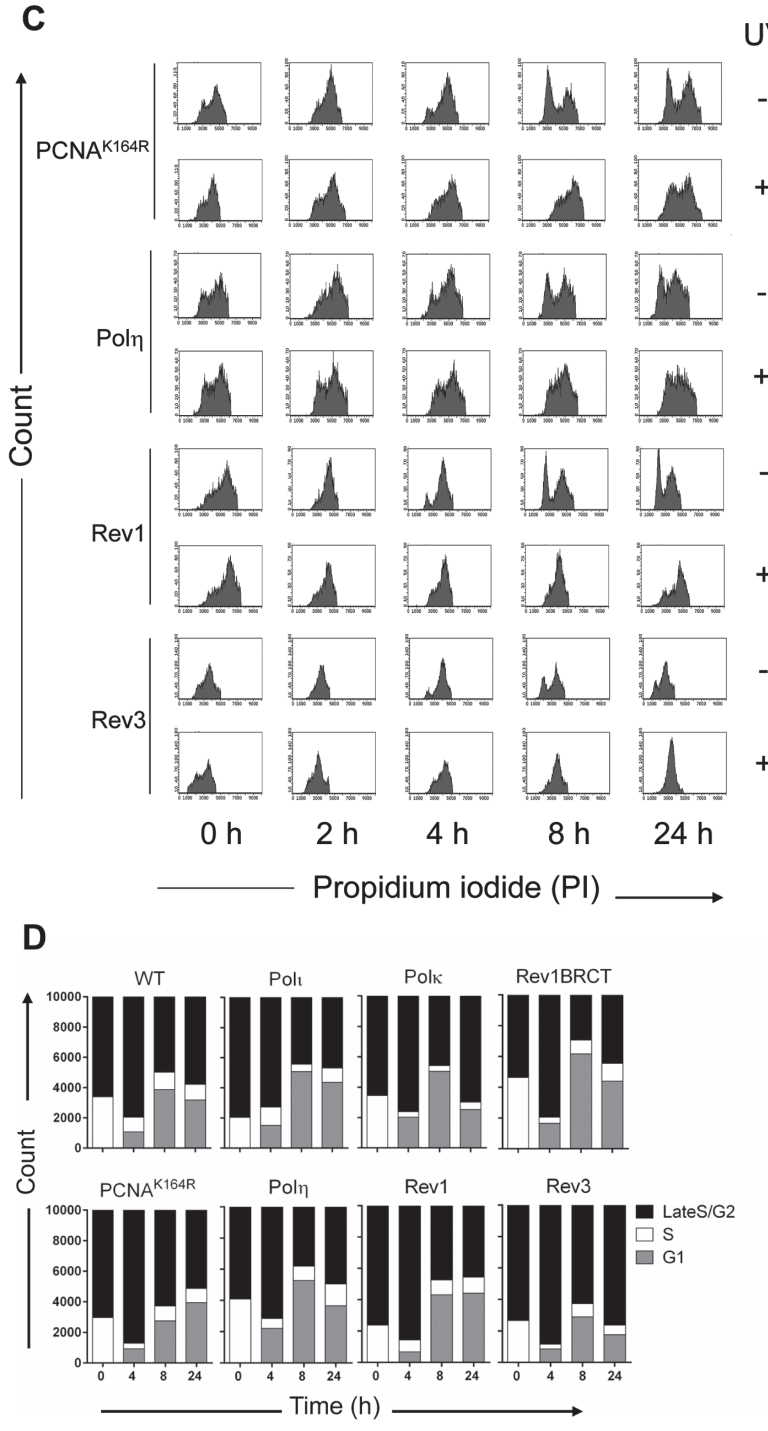

Figure S2 | (***Continued***)

REFERENCES

Andersen PL, Xu F, Ziola B, McGregor WG, Xiao W (2011). Sequential assembly of translesion DNA polymerases at UV-induced DNA damage sites. *Mol Biol Cell*. **22:** *2373-2383*

Arakawa H, Moldovan GL, Saribasak H, Saribasak NN, Jentsch S, Buerstedde JM (2006). A role for PCNA ubiquitination in immunoglobulin hypermutation. *PLoS Biol*. **4:** *e366*

Atkinson J, McGlynn P (2009). Replication fork reversal and the maintenance of genome stability. *Nucleic Acids Res*. **37:** *3475-3492*

Auclair Y, Rouget R, Belisle JM, Costantino S, Drobetsky EA (2010). Requirement for functional DNA polymerase eta in genome-wide repair of UV-induced DNA damage during S phase. *DNA Repair (Amst)*. **9:** *754-764*

Bienko M, Green CM, Crosetto N, Rudolf F, Zapart G, Coull B, Kannouche P, Wider G, Peter M, Lehmann AR *et al.* (2005). Ubiquitin-binding domains in Y-family polymerases regulate translesion synthesis. *Science*. **310:** *1821-1824*

Daigaku Y, Davies AA, Ulrich HD (2010). Ubiquitin-dependent DNA damage bypass is separable from genome replication. *Nature*. **465:** *951-955*

de Feraudy S, Revet I, Bezrookove V, Feeney L, Cleaver JE (2010). A minority of foci or pan-nuclear apoptotic staining of gammaH2AX in the S phase after UV damage contain DNA double-

strand breaks. *Proc Natl Acad Sci U S A*. **107:** *6870-6875*

de Groote FH, Jansen JG, Masuda Y, Shah DM, Kamiya K, de Wind N, Siegal G (2011). The Rev1 translesion synthesis polymerase has multiple distinct DNA binding modes. *DNA Repair (Amst)*. **10:** *915-925*

Delbos F, De Smet A, Faili A, Aoufouchi S, Weill JC, Reynaud CA (2005). Contribution of DNA polymerase eta to immunoglobulin gene hypermutation in the mouse. *J Exp Med*. **201:** *1191-1196*

Diamant N, Hendel A, Vered I, Carell T, Reissner T, de Wind N, Geacinov N, Livneh Z (2012). DNA damage bypass operates in the S and G2 phases of the cell cycle and exhibits differential mutagenicity. *Nucleic Acids Res*. **40:** *170-180*

Dumstorf CA, Clark AB, Lin Q, Kissling GE, Yuan T, Kucherlapati R, McGregor WG, Kunkel TA (2006). Participation of mouse DNA polymerase iota in strand-biased mutagenic bypass of UV photoproducts and suppression of skin cancer. *Proc Natl Acad Sci U S A*. **103:** *18083-18088*

Edmunds CE, Simpson LJ, Sale JE (2008). PCNA ubiquitination and REV1 define temporally distinct mechanisms for controlling translesion synthesis in the avian cell line DT40. *Mol Cell*. **30:** *519-529*

Faili A, Aoufouchi S, Flatter E, Gueranger Q, Reynaud CA, Weill JC (2002). Induction of somatic hypermutation in immunoglobulin genes is dependent on DNA polymerase iota. *Nature*. **419:** *944-947*

Fenech M (1993). The cytokinesis-block micronucleus technique: a detailed description of the method and its application to genotoxicity studies in human populations. *Mutat Res*. **285:** *35-44*

Gueranger Q, Stary A, Aoufouchi S, Faili A, Sarasin A, Reynaud CA, Weill JC (2008). Role of DNA polymerases eta, iota and zeta in UV resistance and UV-induced mutagenesis in a human cell line. *DNA Repair (Amst)*. **7:** *1551-1562*

Guo C, Kosarek-Stancel JN, Tang TS, Friedberg EC (2009). Y-family DNA polymerases in mammalian cells. *Cell Mol Life Sci*. **66:** *2363-2381*

Hendel A, Krijger PH, Diamant N, Goren Z, Langerak P, Kim J, Reissner T, Lee KY, Geacintov NE, Carell T *et al.* (2011). PCNA ubiquitination is important, but not essential for translesion DNA synthesis in mammalian cells. *PLoS Genet*. **7:** *e1002262*

Hoege C, Pfander B, Moldovan GL, Pyrowolakis G, Jentsch S (2002). RAD6-dependent DNA repair is linked to modification of PCNA by ubiquitin and SUMO. *Nature*. **419:** *135-141*

Ikehata H, Ono T (2011). The mechanisms of UV mutagenesis. *J Radiat Res*. **52:** *115-125*

Ito W, Yokoi M, Sakayoshi N, Sakurai Y, Akagi J, Mitani H, Hanaoka F (2012). Stalled Poleta at its cognate substrate initiates an alternative translesion synthesis pathway via interaction with REV1. *Genes Cells*. **17:** *98-108*

Jansen JG, Langerak P, Tsaalbi-Shtylik A, van den Berk P, Jacobs H, de Wind N (2006). Strand-biased defect in C/G transversions in hypermutating immunoglobulin genes in Rev1-deficient mice. *J Exp Med*. **203:** *319-323*

Jansen JG, Tsaalbi-Shtylik A, Hendriks G, Gali H, Hendel A, Johansson F, Erixon K, Livneh Z, Mullenders LH, Haracska L *et al.* (2009a). Separate domains of Rev1 mediate two modes of DNA damage bypass in mammalian cells. *Mol Cell Biol*. **29:** *3113-3123*

Jansen JG, Tsaalbi-Shtylik A, Hendriks G, Verspuy J, Gali H, Haracska L, de Wind N (2009b). Mammalian polymerase zeta is essential for post-replication

repair of UV-induced DNA lesions. *DNA Repair (Amst)*. **8:** *1444-1451*

Jansen JG, Tsaalbi-Shtylik A, Langerak P, Calleja F, Meijers CM, Jacobs H, de Wind N (2005). The BRCT domain of mammalian Rev1 is involved in regulating DNA translesion synthesis. *Nucleic Acids Res*. **33:** *356-365*

Johansson F, Lagerqvist A, Erixon K, Jenssen D (2004). A method to monitor replication fork progression in mammalian cells: nucleotide excision repair enhances and homologous recombination delays elongation along damaged DNA. *Nucleic Acids Res*. **32:** *e157*

Kannouche PL, Wing J, Lehmann AR (2004). Interaction of human DNA polymerase eta with monoubiquitinated PCNA: a possible mechanism for the polymerase switch in response to DNA damage. *Mol Cell*. **14:** *491-500*

Krijger PH, van den Berk PC, Wit N, Langerak P, Jansen JG, Reynaud CA, de Wind N, Jacobs H (2011). PCNA ubiquitination-independent activation of polymerase eta during somatic hypermutation and DNA damage tolerance. *DNA Repair (Amst)*. **10:** *1051-1059*

Langerak P, Nygren AO, Krijger PH, van den Berk PC, Jacobs H (2007). A/T mutagenesis in hypermutated immunoglobulin genes strongly depends on PCNAK164 modification. *J Exp Med*. **204:** *1989-1998*

McDonald JP, Frank EG, Plosky BS, Rogozin IB, Masutani C, Hanaoka F, Woodgate R, Gearhart PJ (2003). 129-derived strains of mice are deficient in DNA polymerase iota and have normal immunoglobulin hypermutation. *J Exp Med*. **198:** *635-643*

Niimi A, Brown S, Sabbioneda S, Kannouche PL, Scott A, Yasui A, Green CM, Lehmann AR (2008). Regulation of proliferating cell nuclear antigen ubiquitination in mammalian cells. *Proc Natl Acad Sci U S A*. **105:** *16125-16130*

Ogi T, Lehmann AR (2006). The Y-family DNA polymerase kappa (pol kappa) functions in mammalian nucleotide-excision repair. *Nat Cell Biol*. **8:** *640-642*

Ogi T, Limsirichaikul S, Overmeer RM, Volker M, Takenaka K, Cloney R, Nakazawa Y, Niimi A, Miki Y, Jaspers NG *et al.* (2010). Three DNA polymerases, recruited by different mechanisms, carry out NER repair synthesis in human cells. *Mol Cell*. **37:** *714-727*

Ohashi E, Murakumo Y, Kanjo N, Akagi J, Masutani C, Hanaoka F, Ohmori H (2004). Interaction of hREV1 with three human Y-family DNA polymerases. *Genes Cells*. **9:** *523-531*

Ohkumo T, Kondo Y, Yokoi M, Tsukamoto T, Yamada A, Sugimoto T, Kanao R, Higashi Y, Kondoh H, Tatematsu M *et al.* (2006). UV-B radiation induces epithelial tumors in mice lacking DNA polymerase eta and mesenchymal tumors in mice deficient for DNA polymerase iota. *Mol Cell Biol*. **26:** *7696-7706*

Okada T, Sonoda E, Yoshimura M, Kawano Y, Saya H, Kohzaki M, Takeda S (2005). Multiple roles of vertebrate REV genes in DNA repair and recombination. *Mol Cell Biol*. **25:** *6103-6111*

Petta TB, Nakajima S, Zlatanou A, Despras E, Couve-Privat S, Ishchenko A, Sarasin A, Yasui A, Kannouche P (2008). Human DNA polymerase iota protects cells against oxidative stress. *EMBO J*. **27:** *2883-2895*

Rogakou EP, Pilch DR, Orr AH, Ivanova VS, Bonner WM (1998). DNA double-stranded breaks induce histone H2AX phosphorylation on serine 139. *J Biol Chem*. **273:** *5858-5868*

Sabbioneda S, Gourdin AM, Green CM, Zotter A, Giglia-Mari G, Houtsmuller A, Vermeulen W, Lehmann AR (2008). Effect of proliferating cell nuclear antigen ubiquitination and chromatin structure on the dynamic properties of the Y-family DNA polymerases. *Mol Biol Cell*. **19:** *5193-5202*

Schmutz V, Janel-Bintz R, Wagner J, Biard D, Shiomi N, Fuchs RP, Cordonnier AM (2010). Role of the ubiquitin-binding domain of Poleta in Rad18-independent translesion DNA synthesis in human cell extracts. *Nucleic Acids Res*. **38:** *6456-6465*

Shachar S, Ziv O, Avkin S, Adar S, Wittschieben J, Reissner T, Chaney S, Friedberg EC, Wang Z, Carell T *et al.* (2009). Two-polymerase mechanisms dictate error-free and error-prone translesion DNA synthesis in mammals. *EMBO J*. **28:** *383-393*

Sharma S, Hicks JK, Chute CL, Brennan JR, Ahn JY, Glover TW, Canman CE (2012). REV1 and polymerase zeta facilitate homologous recombination repair. *Nucleic Acids Res*. **40:** *682-691*

Simpson LJ, Sale JE (2003). Rev1 is essential for DNA damage tolerance and non-templated immunoglobulin gene mutation in a vertebrate cell line. *EMBO J*. **22:** *1654-1664*

Smits VA, Warmerdam DO, Martin Y, Freire R (2010). Mechanisms of ATR-mediated checkpoint signalling. *Front Biosci (Landmark Ed)*. **15:** *840-853*

Stelter P, Ulrich HD (2003). Control of spontaneous and damage-induced mutagenesis by SUMO and ubiquitin conjugation. *Nature*. **425:** *188-191*

Szuts D, Marcus AP, Himoto M, Iwai S, Sale JE (2008). REV1 restrains DNA polymerase zeta to ensure frame fidelity during translesion synthesis of UV photoproducts in vivo. *Nucleic Acids Res*. **36:** *6767-6780*

Temviriyanukul P, Meijers M, van Hees-Stuivenberg S, Boei JJ, Delbos F, Ohmori H, de Wind N, Jansen JG (2012). Different sets of translesion synthesis DNA polymerases protect from genome instability induced by distinct food-derived genotoxins. *Toxicol Sci*. **127:** *130-138*

Tissier A, Kannouche P, Reck MP, Lehmann AR, Fuchs RP, Cordonnier A (2004). Co-localization in replication foci and interaction of human Y-family members, DNA polymerase pol eta and REVl protein. *DNA Repair (Amst)*. **3:** *1503-1514*

Tsaalbi-Shtylik A, Verspuy JW, Jansen JG, Rebel H, Carlee LM, van der Valk MA, Jonkers J, de Gruijl FR, de Wind N (2009). Error-prone translesion replication of damaged DNA suppresses skin carcinogenesis by controlling inflammatory hyperplasia. *Proc Natl Acad Sci U S A*. **106:** *21836-21841*

Van Sloun PP, Jansen JG, Weeda G, Mullenders LH, van Zeeland AA, Lohman PH, Vrieling H (1999). The role of nucleotide excision repair in protecting embryonic stem cells from genotoxic effects of UV-induced DNA damage. *Nucleic Acids Res*. **27:** *3276-3282*

Van Sloun PP, Varlet I, Sonneveld E, Boei JJ, Romeijn RJ, Eeken JC, De Wind N (2002). Involvement of mouse Rev3 in tolerance of endogenous and exogenous DNA damage. *Mol Cell Biol*. **22:** *2159-2169*

Watanabe K, Tateishi S, Kawasuji M, Tsurimoto T, Inoue H, Yamaizumi M (2004). Rad18 guides poleta to replication stalling sites through physical interaction and PCNA monoubiquitination. *EMBO J*. **23:** *3886-3896*

Waters LS, Minesinger BK, Wiltrout ME, D'Souza S, Woodruff RV, Walker GC (2009). Eukaryotic translesion polymerases and their roles and regulation in DNA damage tolerance. *Microbiol Mol Biol Rev*. **73:** *134-154*

White DE, Negorev D, Peng H, Ivanov AV, Maul GG, Rauscher FJ, 3rd (2006). KAP1, a novel substrate for PIKK family members, colocalizes with numerous damage response factors at DNA lesions. *Cancer Res*. **66:** *11594-11599*

Wittschieben JP, Reshmi SC, Gollin SM, Wood RD (2006). Loss of DNA polymerase zeta causes chromosomal instability in mammalian cells. *Cancer Res*. **66:** *134-142*

Yagi T, Nikaido O, Takebe H (1984). Excision repair of mouse and human fibroblast cells, and a factor affecting the amount of UV-induced unscheduled DNA synthesis. *Mutat Res*. **132:** *101-112*

Yoon JH, Prakash L, Prakash S (2009). Highly error-free role of DNA polymerase eta in the replicative bypass of UV-induced pyrimidine dimers in mouse and human cells. *Proc Natl Acad Sci U S A*. **106:** *18219-18224*

Yoon JH, Prakash L, Prakash S (2010). Error-free replicative bypass of (6-4) photoproducts by DNA polymerase zeta in mouse and human cells. *Genes Dev*. **24:** *123-128*

Zhang Y, Yuan F, Wu X, Wang M, Rechkoblit O, Taylor JS, Geacintov NE, Wang Z (2000). Error-free and error-prone lesion bypass by human DNA polymerase kappa in vitro. *Nucleic Acids Res*. **28:** *4138-4146*

Ziv O, Geacintov N, Nakajima S, Yasui A, Livneh Z (2009). DNA polymerase zeta cooperates with polymerases kappa and iota in translesion DNA synthesis across pyrimidine photodimers in cells from XPV patients. *Proc Natl Acad Sci U S A*. **106:** *11552-11557*

Ziv Y, Bielopolski D, Galanty Y, Lukas C, Taya Y, Schultz DC, Lukas J, Bekker-Jensen S, Bartek J, Shiloh Y (2006). Chromatin relaxation in response to DNA double-strand breaks is modulated by a novel ATM- and KAP-1 dependent pathway. *Nat Cell Biol*. **8:** *870-876*